Instantaneous Velocity Profiles during Granular Avalanches

Sylvain Courrech du Pont,[1,2] Raphaël Fischer,[1] Philippe Gondret,[1] Bernard Perrin,[3] and Marc Rabaud[1]

[1]*Laboratoire Fluides, Automatique, Systèmes Thermiques (UMR CNRS 7608), Bâtiment 502, Campus Universitaire, 91405 Orsay Cedex, France*

[2]*School of Mathematics, University of Bristol, University Walk, Bristol BS8 1TW, United Kingdom*

[3]*Laboratoire Pierre Aigrain (UMR CNRS 8551), 24, rue Lhomond, 75231 Paris Cedex, France*

(Received 25 June 2004; published 3 February 2005)

We perform experimental measurements of the instantaneous velocity profile of the flowing layer during granular avalanches. In the pile depth, the velocity profile follows a pure exponential decrease in contrast with steady flows that are known to exhibit a well developed upper linear part. The velocity profile in the pile width is a plug flow with two exponential boundary layers at the walls. Even though no steady state is observed during the avalanche, these velocity profiles are self-similar and build up almost instantaneously, with time independent characteristic lengths.

DOI: 10.1103/PhysRevLett.94.048003 PACS numbers: 45.70.Ht

Disordered systems such as granular materials [1], but also foams [2], or concentrated emulsions and suspensions [3], exhibit rheological properties that cannot be understood within the scope of standard solid or liquid mechanics. For such athermal systems, a solidlike state is observed at small stresses, and it is only beyond a critical stress that a macroscopic flow arises. As the deformation or deformation rate is nonlinear with the stress, the flow of such systems can be very complex even in very simple configurations. Indeed, the spontaneous localization of the strain in narrow regions (the so-called ''shear banding'') in the bulk or at the surface of the materials is often observed. The shear banding phenomenon controls most of the practical situations encountered in industrial handling of grains (agriculture, pharmacology, etc.) and in geophysical problems (sand dunes migration, pyroclastic flows, etc.). In the case of a granular pile, an important challenge is the understanding of the transient avalanche flow localized at the pile surface that leads a dense granular pile from solid (static) to liquid (flowing) state and vice versa. The many experimental studies held for some years have all found that granular piles dynamics do not follow the predicted self-organized criticality behavior [4] as the amplitude of avalanches is not power law distributed but of well defined mean value [5]. This mean amplitude proceeds from a hysteretic behavior between two angles, the so-called maximum angle of stability θ_m at which an avalanche starts spontaneously and the angle of repose θ_r at which the avalanche stops. Two different ways of investigation appeared recently: one that focuses on the avalanche front dynamics [6,7] and another one interested in the velocity profiles for the steady regime of granular surface flows [8–13]. But to date no detailed time evolution of the velocity profile in the evolving flowing layer is available for the complete transient avalanche process. In the special case of steady surface flows where averaging is possible, measurements at the sidewall of the grain velocity profile in the depth of a pile have been performed recently either by continuously feeding an open pile from the top [9,12] or by rotating a partially filled drum at a sufficient angular velocity [10,11]. In these steady cases, grains flow at a constant dynamic pile angle and with a velocity that decreases from the pile surface down to the depth in two different parts. In the ''flowing layer'' just below the surface, the velocity profile is found linear with a constant shear rate that scales as $(g/d)^{1/2}$, where g stands for gravity and d for the grain diameter [8,10,13]. Below this flowing layer exists a so-called ''creeping flow'' characterized by an exponential velocity decrease with a characteristic length of a few grain diameters [9,10,13]. These two behaviors can be recovered in different theroretical models [14] that invoke nonlocality, trapping, or dilatancy effects. In contrast with all these steady state studies, the aim of this Letter is to present the evolution of the instantaneous grain velocity profile during the time duration of discrete avalanches. Such a study is important as the precise form of the velocity profile in the flowing layer is crucial for predicting correctly unsteady granular flows [15]. Our measurements show that the instantaneous velocity profile is a pure exponential decrease in the pile depth with a time independent characteristic length of a few beads throughout the avalanches. No linear velocity profile is observed and discrete avalanches never reach any steady regime. Finally, we show that the sole visualization from the side and from the top of the pile allows us to describe the entire 3D velocity field.

Our setup consists of a horizontal rotating drum closed by two glass walls allowing visualization. The inner diameter D of the drum has been varied between 17 and 50 cm, and its length b between 1.5 and 7.5 cm (inset of Fig. 1). The drum is half filled with dry sieved solid glass spheres of density $\rho_s = 2.5\ \mathrm{g/cm^3}$ and of diameter d ranging from 0.2 to 3 mm. For the results presented here, mainly $D = 17\,\mathrm{cm}$, $b = 2.5\,\mathrm{cm}$, and $d = 0.95 \pm 0.05\,\mathrm{mm}$. The rotation rate of the drum, ensured by a microstep motor (see Refs. [16–18] for details), was low enough

($\Omega \sim 10^{-3}$ rpm) for the granular flow to be intermittent [19–21]: The pile slope θ increases linearly with time at the rate Ω, then quickly relaxes by a surface avalanche process that lasts roughly 1 s [16,17]. Two video cameras are used simultaneously. With one classical video camera (25 images/s) aligned along the cylinder axis, we view the entire pile from the side. We observe no front propagation in the avalanche duration, the pile interface remains flat, which allows the study of the time evolution of the pile angle θ [16–18]. An example of such evolution from θ_m to θ_r is displayed in Fig. 1. With one high-speed digital video camera (FASTCAM Super 1000) either aligned along the horizontal cylinder axis (Oy) or perpendicular to the pile surface (Oz), zoomed images (windows of typically 20 grain diameter long) of the pile around the cylinder center ($x = 0$) are taken from the side or from above at the sampling rate of 500 images/s with the resolution 240 × 256 pixels. The correlation of small boxes (8 × 8 pixels) between two successive images using a particle image velocimetry algorithm (Davis software, LaVision) allows us to calculate the velocity field of the flowing grains. This box size is adjusted to resolve spatial variations of the velocity profile down to the grain size. We here focus on the velocity component u along the pile interface (x axis) corresponding to the main flow direction. Each velocity field $u(x, y$ or $z, t)$ is then averaged over the 20 d window size along the flow x direction to obtain the velocity field $u(y$ or $z, t)$ at each time t along the y (pile width) or z (pile depth) direction in the plane $x = 0$. Accordingly the velocity resolution is better than 1 mm/s. Typical velocity profiles obtained from the side and from above are displayed superimposed to the pile images in Figs. 2(a) and 2(b), respectively. The velocity decreases rapidly along the depth [Fig. 2(a)] with a typical flowing layer of a few bead diameters. The transverse velocity profile [Fig. 2(b)] presents a maximum at midgap and a large slip at the walls. We will see that during the avalanche the velocity profiles in the depth and in the width remain both invariant in shape with a maximum evolving value.

The evolution of the velocity profiles measured at successive times of a typical avalanche are displayed in Figs. 3 and 4. The data $u_w(z, t)$ of the velocity at the wall in the depth are shown in Fig. 3. Their representation in the lin-log plot (see the inset) along remarkable parallel straight lines demonstrates that the in-depth velocity decrease is exponential with the same characteristic length $\lambda \simeq 2.2$ mm. Thus the velocity profile at the wall may be written as $u_w(z, t) = u_{w0}(t)\exp(-z/\lambda)$, where $z = 0$ corresponds at each instant to the pile surface position and u_{w0} stands for the surface velocity at the wall. Let us emphasize that the successive avalanches have different amplitude $\theta_m - \theta_r$ and time evolution $\theta(t)$, but the velocity profile is always exponential and its characteristic length averaged over 20 avalanches is $\lambda = 2.4 \pm 0.3$ mm. Preliminary studies for different bead diameters ($0.2 < d < 3$ mm) indicate that λ scales with d as $\lambda/d = 3 \pm 1$. On the other hand, the λ value remains constant within 10% when varying either the pile width b ($2 < b < 7.5$ cm, $10 < b/d < 75$) or the pile length D ($17 < D < 50$ cm, $100 < D/d < 500$). Let us note that this characteristic length $\lambda \simeq 3d$ is consistent with the one already found for the exponential part of the velocity profile in *steady* regimes [9,10,13].

In Fig. 4, the surface velocity profiles in the width, $u_s(y, t)$, are curved symmetrically with a maximum value u_{s0} at midway ($y = 0$) and a large slip value u_{w0} at the walls ($y = \pm b/2$), more than half u_{s0}. When normalized with the gap averaged value $\langle u_s(y, t)\rangle_y$, all these profiles collapse well onto a single master curve. We also check the form invariance of the velocity profile in the width by calculating the ratio of the gap averaged surface velocity $\langle u_s(y, t)\rangle_y$ to the surface velocity at the wall $u_{w0}(t)$. This ratio remains constant at any time of the avalanche, with the value $\langle u_s(y, t)\rangle_y / u_{w0}(t) = 1.5 \pm 0.1$. This experiment and other experiments with different gap values ($25 < b/d < 150$) show that the velocity profile in the width at

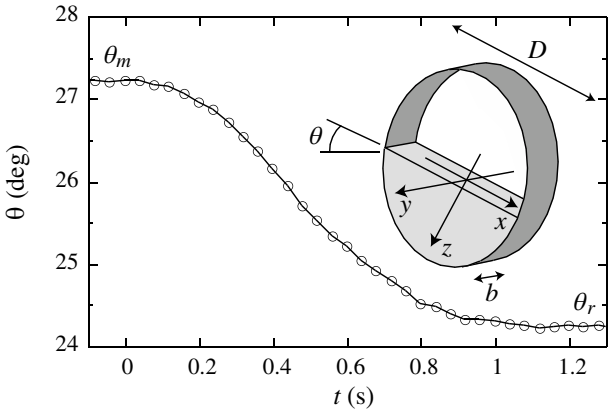

FIG. 1. Time evolution during an avalanche of the slope angle θ of a pile of dry glass beads of diameter $d = 0.95$ mm located in a rotating drum of diameter $D = 17$ cm and length $b = 2.5$ cm. Inset: sketch of the setup with the axis orientation.

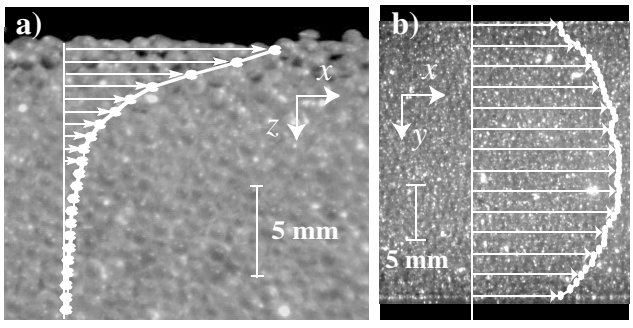

FIG. 2. Typical pile images and velocity profile u_w at the wall in the pile depth (a) and u_s at the pile surface in the pile width between the walls (b) at one instant of a granular avalanche ($t = 0.5$ s, $u_{w0} = 70$ mm/s, $d = 0.95$ mm, $b = 2.5$ cm, and $D = 17$ cm).

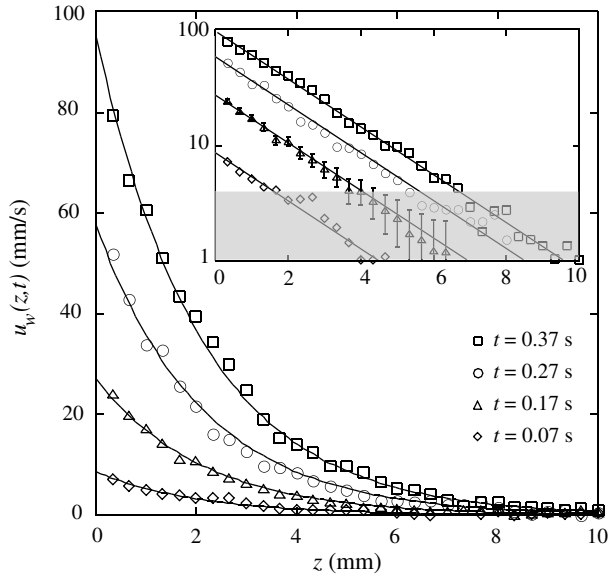

FIG. 3. Velocity profile at the wall $u_w(z, t)$ along the pile depth z at successive times t of an avalanche. Continuous lines correspond to exponential fits with *the same* $\lambda = 2.2$ mm. The inset is the corresponding semilog plot. In the gray area ($u_w < 4$ mm/s), errors bars are larger than 25%.

the pile surface can be considered empirically as the sum of two exponential terms $\exp[(y \pm b/2)/\Lambda]$ that can be ascribed to each wall effect with the characteristic length $\Lambda \simeq 8$ mm. The corresponding profile may be written as $u_s(y) = A + B\cosh(y/\Lambda)$, where A and B are related to the velocity values at the wall u_{w0} and at midgap u_{s0}, and to the ratio b/Λ. This plug flow resembles the one observed in vertical chute flows with a slip at the wall depending on the wall roughness, two boundary layers at the walls, and a flat core [13]. The characteristic length Λ found here is quite similar to the chute flow value of 5–6 d and significantly higher than λ, suggesting that different mechanisms are involved: dilatancy and gravity trapping for λ, and wall effect for Λ.

Let us now look at Fig. 5 to the precise time evolution of the velocity at the wall (its surface value u_{w0} and its characteristic length λ) together with the grain flow rate $Q(t)$. In Fig. 5(a), the time evolution of the surface velocity at the wall $u_{w0}(t)$ shows that there is no plateau but a quick increase from zero towards the maximum value (here $u_{w0\,\max} \sim 80$ mm/s) followed by a smoother decrease towards zero. Note that the maximum of the surface velocity corresponds to the inflection point in the time evolution of the pile angle (Fig. 1). It is worth noting that although the velocity profiles remain time invariant in form both in the depth and in the width, the surface velocity does not reach any steady state during the avalanche. As soon as the velocity is significantly nonzero [Fig. 5(a)], the characteristic length λ (the typical flowing layer thickness) is well defined [Fig. 5(b)]. By contrast to the unsteady behavior of the velocity, the characteristic length λ is constant all along the avalanche duration, except a slight decrease at the end. This constant value $\lambda \sim 2$ mm builds up very rapidly, roughly in the elementary fall characteristic time $(d/g)^{1/2} \sim 10^{-2}$ s, as already shown in Fig. 3 for

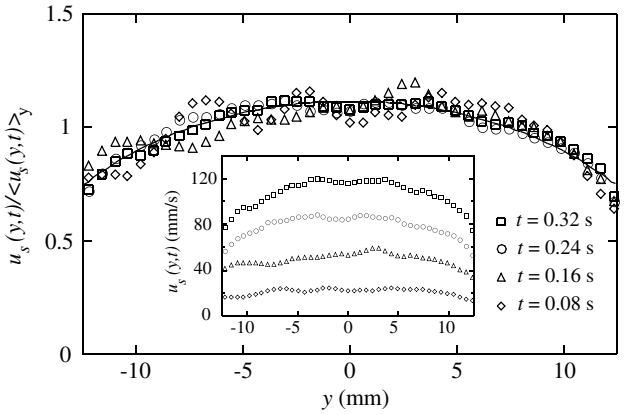

FIG. 4. Surface velocity profile $u_s(y, t)$, normalized or not (see the inset) by its gap averaged value $\langle u_s(y, t)\rangle_y$, in the pile width at successive times t of an avalanche. The continuous line corresponds to a hyperbolic cosine fit with $\Lambda = 8$ mm.

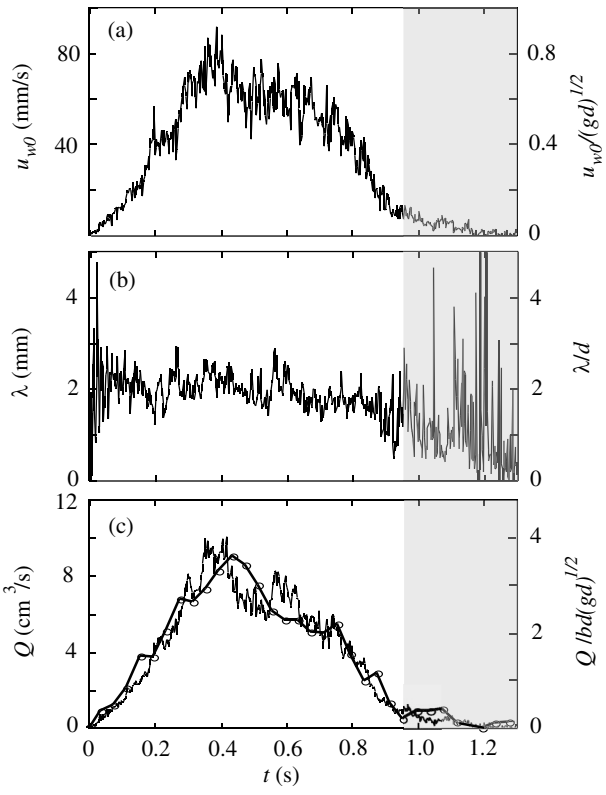

FIG. 5. Time evolution during the avalanche of Fig. 1 for (a) the surface velocity at the wall u_{w0}, (b) the characteristic flowing layer λ, and (c) the instantaneous grain flow rate Q calculated either from velocity profile measurements (Q_u, thin continuous line) or from pile angle measurements (Q_θ, thick continuous line with data points).

$t = 0.07$ s. The maximum velocity gradient (shear rate) reached during the avalanche is $1.5 \times u_{w0\,\max}/\lambda \simeq 60\ \mathrm{s}^{-1}$, which is close to but smaller than the constant shear rate value $(g/d)^{1/2} \sim 100\ \mathrm{s}^{-1}$ observed in the linear profiles of steady surface flows. The fact that this ''critical shear rate value'' is not overtaken is coherent with the fact that we do not observe any linear part in the velocity profile of our discrete avalanches.

The instantaneous grain flow rate $Q(t)$ at midslope ($x = 0$) can be calculated by two ways. The first way consists of integrating the instantaneous velocity profiles in the depth and in the width to obtain the grain flow rate $Q_u(t) = \int u(y, z, t)dydz$. The second way consists of differentiating the instantaneous pile angle with respect to time (Fig. 1) in order to obtain the grain flow rate $Q_\theta(t) = -(D^2b/8)(d\theta/dt)$ [20]. These two grain flow rates plotted in Fig. 5(c) superimpose very well, meaning that the in-depth exponential velocity profile measured at the wall stands in the bulk of the material with the same λ for all in-gap positions y. Thus surface measurements (from the side and from the top) are here sufficient to catch the in-bulk behavior without resorting to technics such as magnetic resonance imaging that are more difficult to use. Note that Q_u [Fig. 5(c)] has the same time evolution as u_{w0} [Fig. 5(a)] since $Q_u(t) = 1.5\lambda b u_{w0}(t)$. Such a time evolution means that the granular avalanche behaves as an accelerating then decelerating rush and that no steady state is reached at any time. This rush motion occurs in Fig. 5 for $0 < t < 0.95$ s. For $t > 0.95$ s (gray zone), the vanishing flow rate corresponds to residual motion of surface grains for which λ is no more defined. Current studies show that the results presented here are not specific to the drum center ($x = 0$) but are similar whatever the streamwise position along the pile (x axis), with a streamwise evolution of the instantaneous grain flux which is maximal at the drum center and zero at the up and down end walls ($x = \pm D/2$).

By conclusion, in contrast with the steady pile surface flows, we have shown that the in-depth instantaneous velocity profile during transient dry granular avalanches is a pure exponential decrease with a characteristic length λ that builds up very rapidly (in a time of the order of few $\sqrt{d/g} \simeq 10^{-2}$ s) and that remains constant during the avalanche. For steady surface flows (continuous avalanching), the linear part of the velocity profile above the exponential part is known to decrease in size as the imposed grain flow rate is reduced [10,13]. One may conclude that this linear part does not appear anymore for nonsteady flows. In the ''natural'' avalanche regime, the grain flow rate is no more imposed but is selected by the system itself. The self-similarity of the velocity profiles we found both in the depth and in the width during the avalanche is surprising as no steady regime is observed. This unsteady character of dry granular avalanches is, however, consistent with the $D^{1/2}$—rather than D—avalanche duration scaling found in either experimental [17] or numerical [22] studies.

This work is supported by the ACI ''Jeunes Chercheurs,'' ACI ''Catastrophes Naturelles'' 2178 of the French Ministry of Research, and GDR MiDi. We thank Niels Vandecasteele for his experimental help and Daniel Bonamy for warm and fruitful discussions.

[1] J. Duran, *Sand, Powders, and Grains* (Springer, New York, 2000).
[2] G. Debregeas, H. Tabuteau, and J.-M. di Meglio, Phys. Rev. Lett. **87**, 178305 (2001).
[3] P. Coussot *et al.*, Phys. Rev. Lett. **88**, 218301 (2002).
[4] P. Bak, C. Tang, and K. Wiesenfeld, Phys. Rev. Lett. **59**, 381 (1987).
[5] P. Evesque and J. Rajchenbach, C R Acad Sci, Ser. 2 **307**, 223 (1988); H. M. Jaeger, C.-H. Liu, and S. R. Nagel, Phys. Rev. Lett. **62**, 40 (1989).
[6] S. Douady *et al.*, Adv. Complex Syst. **4**, 509 (2001).
[7] J. Rajchenbach, Phys. Rev. Lett. **88**, 014301 (2002).
[8] J. Rajchenbach, Adv. Phys. **49**, 229 (2000).
[9] T. S. Komatsu *et al.*, Phys. Rev. Lett. **86**, 1757 (2001).
[10] D. Bonamy, F. Daviaud, and L. Laurent, Phys. Fluids **14**, 1666 (2002).
[11] N. Jain, J. M. Ottino, and R. M. Lueptow, Phys. Fluids **14**, 572 (2002).
[12] N. Taberlet *et al.*, Phys. Rev. Lett. **91**, 264301 (2003).
[13] GDR MiDi, Eur. Phys. J. E **14**, 341 (2004).
[14] D. Bonamy and P. Mills, Europhys. Lett. **63**, 42 (2003); B. Andreotti and S. Douady, Phys. Rev. E **63**, 031305 (2001); J. Rajchenbach, Phys. Rev. Lett. **90**, 144302 (2003); C. Josserand, P.-Y. Lagrée, and D. Lhuillier, Eur. Phys. J. E **14**, 127 (2004).
[15] A. Aradian, E. Raphaël, and P.-G. de Gennes, Phys. Rev. E **60**, 2009 (1999).
[16] S. Courrech, Ph.D. thesis, Université Paris-Sud, 2003.
[17] S. Courrech du Pont *et al.*, Phys. Rev. Lett. **90**, 044301 (2003).
[18] S. Courrech du Pont *et al.*, Europhys. Lett. **61**, 492 (2003).
[19] J. Rajchenbach, Phys. Rev. Lett. **65**, 2221 (1990).
[20] M. Caponeri *et al.*, in *Mobile Particulate Systems*, edited by E. Guazzelli and L. Oger (Kluwer Academic Publishers, Dordrecht, 1994), pp. 331–336.
[21] P.-A. Lemieux and D. J. Durian, Phys. Rev. Lett. **85**, 4273 (2000).
[22] C. M. Dury, Ph.D. thesis, Philipps-Universitat Marburg, 1999; G. H. Ristow, *Pattern Formation in Granular Materials* (Springer-Verlag, New York, 2000).